



# Computational Chemistry

How to cite: Angew. Chem. Int. Ed. 2023, e202307379 doi.org/10.1002/anie.202307379

# Tetra-*tert*-butyl-s-indacene is a Bond-Localized $C_{2h}$ Structure and a Challenge for Computational Chemistry

Lucas J. Karas<sup>+</sup>, Said Jalife<sup>+</sup>, Renan V. Viesser, João V. Soares, Michael M. Haley,\* and Judy I. Wu\*

**Abstract:** Whether tetra-*tert*-butyl-s-indacene is a symmetric  $D_{2\rm h}$  structure or a bond-alternating  $C_{2\rm h}$  structure remains a standing puzzle. Close agreement between experimental and computed proton chemical shifts based on minima structures optimized at the M06-2X,  $\omega$ B97X-D, and M11 levels confirm a bond-localized  $C_{2\rm h}$  symmetry, which is consistent with the expected strong antiaromaticity of TtB-s-indacene.

Tetra-tert-butyl-s-indacene (TtB-s-indacene) represents one of the first few critical examples of a kinetically trapped antiaromatic compound.[1,2] It is expected to have a bond localized  $C_{2h}$  structure, resulting from antiaromaticity of the planar, cyclic, 12 π-electron conjugated core, but a large number of experimental and theoretical works indicate a possible bond delocalized  $D_{\mathrm{2h}}$  structure. [3-9] Unsubstituted sindacene, first prepared in 1963, [10] decomposes readily and no structural data could be acquired. Hafner later prepared TtB-s-indacene in 1986 showing that while the compound still was sensitive to oxygen and traces of acid in solution, it could be obtained as red needles that were air stable in the solid state. [1,2] Consistent with its antiaromatic character, <sup>1</sup>H NMR spectra of TtB-s-indacene revealed upfield shifted ring protons compared to those of a non-aromatic methyldihydro derivative (Figure 1).

The exact structure of TtB-s-indacene nonetheless was difficult to determine. The presence of four peaks in the  $^{13}$ C NMR spectrum at  $-130\,^{\circ}$ C for the twelve ring C atoms could point to either a completely delocalized  $12\,\pi$ -electron system or a low energy barrier between two valence isomers. Evidence from X-ray data, both at room temperature and at  $100\,\mathrm{K}$ , indicated a symmetric  $D_{2\mathrm{h}}$  structure,  $^{[2,4]}$  yet the possible roles of residual disorder could not be ruled out. It was suggested that the crystal structure of TtB-s-indacene

[\*] Dr. L. J. Karas,\* Dr. S. Jalife,\* Dr. R. V. Viesser, J. V. Soares, Prof. J. I. Wu Department of Chemistry, University of Houston Houston, TX 77204 (USA)

E-mail: jiwu@central.uh.edu Prof. M. M. Halev

Department of Chemistry & Biochemistry and the Materials Science Institute, University of Oregon

Eugene, OR 97403-1253 (USA) E-mail: haley@uoregon.edu

[+] These authors contributed equally to this work.

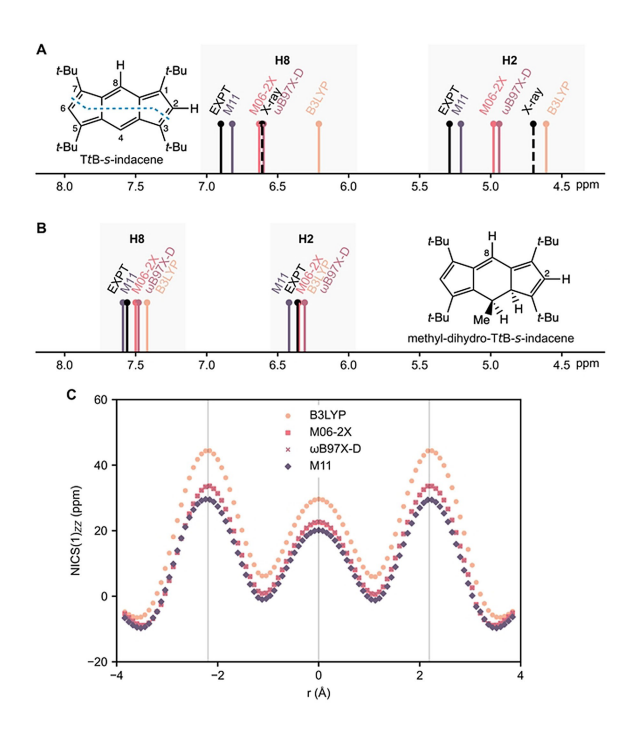


Figure 1. Experimental <sup>1</sup>H NMR (data from reference [2]) and computed proton chemical shifts for H8 and H2 in A) TtB-s-indacene (H8: 6.90 ppm, H2: 5.29 ppm, expt.) and B) methyl-dihydro-TtB-s-indacene (H8: 7.56 ppm, H2: 6.36 ppm, expt.). Proton chemical shifts were computed at B97-2/6-311 + G(d,p) for minima geometries optimized at the B3LYP, M06-2X, ωB97X-D and M11/6-311 + G(d,p) levels and for a partially optimized X-ray structure (see footnote [e], Table 1). C) NICS-XY-scans for TtB-s-indacene at B97-2/6-311 + G(d,p), based B3LYP, M06-2X, ωB97X-D, and M11/6-311 + G(d,p) geometries. Note overlapping M06-2X and ωB97X-D scans.

might be a "frozen transition state structure" resulting from solid-state packing and thus did not necessarily reflect its symmetry as a free molecule. We now show that TtB-s-indacene indeed has a bond localized  $C_{2h}$  structure as expected by its antiaromaticity.

Although early Hückel molecular orbital theory and semiempirical calculations predicted a  $C_{2h}$  structure for unsubstituted s-indacene, [5,11,12] Koch et al. concluded based on ab initio and density functional theory (DFT) calculations that agreement between the computed  $D_{2h}$  structure of s-indacene and the X-ray structure of TtB-s-indacene must mean that TtB-s-indacene is a "completely delocalized 12  $\pi$ -electron system".[6,7] MP2/6-31G(d) calculations for s-indacene found the  $C_{2h}$  structure to be lower in energy than the





 $D_{2h}$  structure by 0.7 kcal/mol, but single point calculations at the CASPT2 level indicated a lower energy  $D_{2h}$  structure by 3.1 kcal/mol. [6] At the LDA and LDA + BP levels, only a  $D_{2h}$ minimum could be located. [6] Subsequent studies performed for unsubstituted s-indacene based on various DFT computations were indecisive. B3LYP/6-31G(d) calculations predicted a "quasi-delocalized" structure. [8] The  $C_{2h}$  structure is a minimum and is 0.1 kcal/mol lower in energy than the  $D_{2h}$ form, which is a transition state structure; however, zeropoint energy correction reverses the relative energy, and the  $D_{2h}$  form becomes 0.6 kcal/mol lower. BLYP predicted a bond localized  $C_{2h}$  structure.<sup>[7]</sup> Heilbronner and Yang,<sup>[3]</sup> and later Salvi et al., [5] recognized that TtB-s-indacene exhibits a stronger tendency towards bond delocalization than the parent s-indacene, but neither provided conclusive evidence for a  $D_{2h}$  geometry. Since X-ray structures can be influenced by crystal packing as well as static and dynamic disorders even at low temperatures, agreement with X-ray data does not provide decisive evidence for the structure of TtB-sindacene. Proton chemical shifts, however, can show large responses even to subtle geometric variations.

Excellent agreement between computed and experimental proton chemical shifts can be found only when the expected geometries are correct. Bühl and Schleyer examined the reported chemical shifts for many boranes, carboranes, and nonclassical carbocations, revealing numerous structural misassignments and finding that computed and experimental proton chemical shifts match only when the assigned geometries were correct. [13] For example, [18] annulene was expected to have a symmetric  $D_{6h}$ structure for over four decades; however, experimental match to ab initio NMR data identified the correct  $C_2$ symmetry.[14] Whereas the computed proton chemical shifts of  $D_{6h}$  [18] annulene structures at various DFT levels were in gross disagreement with experiment, [15,16] the computed averaged proton chemical shifts of  $C_2$  minima geometries of [18] annulene at the KMLYP (outer: 8.9 ppm, inner: -2.5 ppm) and BHLYP (outer: 9.2 ppm, inner: -2.8 ppm) levels matched closely with experiment (outer: 9.3 ppm, inner: -3.0 ppm). Using the same approach, computed proton chemical shifts for a partially optimized X-ray geometry of TtB-s-indacene (H8: 6.61 ppm, H2: 4.70 ppm, black dashed line, see also Table 1, footnote [e]) shows signals far upfield from the reported experimental <sup>1</sup>H NMR shifts (H8: 6.90 ppm, H2: 5.29 ppm, black solid line, Figure 1A).  $^{[1,2]}$  TtB-s-indacene cannot have a symmetric  $D_{2h}$ structure!

Proton chemical shifts computed at B97-2/6-311 + G(d,p) for minima geometries of TtB-s-indacene obtained at the B3LYP (H8: 6.20 ppm, H2: 4.60 ppm,  $D_{2h}$ ), M06-2X (H8: 6.62 ppm, H2: 4.97 ppm,  $C_{2h}$ ),  $\omega$ B97X-D (H8: 6.59 ppm, H2: 4.93 ppm,  $C_{2h}$ ), and M11 (H8: 6.81 ppm, H2: 5.20 ppm,  $C_{2h}$ ) levels spread over a range of 0.61 ppm for H8 and 0.60 ppm for H2 (cf. H8: 6.90 ppm, H2: 5.29 ppm, expt., see Figure 1A). Computed proton chemical shifts based on B3LYP-D3 geometries are close to the B3LYP values and are included in the Supporting Information. The M11 structure displays the most bond length alternation ( $\Delta$ r=0.086 Å, see footnote [c] in Table 1, cf. values for other functionals) and

**Table 1:** Computed C–C bond length difference  $(\Delta r)$ , and relative free energies  $(\Delta G_{\rm rel})$  between the  $C_{2h}$  and  $D_{2h}$  structures of TtB-s-indacene at the B3LYP, M06-2X,  $\omega$ B97X-D, and M11/6-311 + G(d,p) levels.

Level	HF <sup>[a]</sup> [%]	PG <sup>[b]</sup>	Δr <sup>[c]</sup> [Å]	$\Delta E_{ m rel}$ [kcal/mol]	$\delta$ H8 $^{ ext{[d]}}$	$\delta$ H2 <sup>[d]</sup> [ppm]
B3LYP	20	$C_{2h}$	_	_	_	_
		$D_{2h}$	0	0.00	6.20	4.60
M06-2X	54	$C_{2h}$	0.066	0.00	6.62	4.97
		$D_{2h}$	0	0.30	6.32	4.60
$\omega$ B97X-D	SR:22	$C_{2h}$	0.069	0.00	6.59	4.93
	LR:100 ω:0.20	$D_{2h}$	0	0.57	6.26	4.53
M11	SR:42.8	$C_{2h}$	0.086	0.00	6.81	5.20
	LR:100 ω:0.25	$D_{2h}$	0	1.80	6.40	4.67
X-ray <sup>[e]</sup>	— —	$D_{2h}$	0.001	_	6.61	4.70

[a] Short range (SR) and long range (LR) percentages of HF exchange. [b] Point Group. [c]  $\Delta r$  is the difference between the two C–C bond lengths of the central six-membered ring connected to C4/C8. [d] Proton chemical shifts were computed at B97-2/6-311+G(d,p) using the computed chemical shielding for hydrogen in benzene as a reference. [e] Based on X-ray crystal structure at 100 K (reference [4]). All ring C–C bonds and the four C–C<sub>I-butyl</sub> bonds were fixed to reported X-ray data, all other parameters were optimized at M11/6-311+G(d,p).

the computed proton chemical shifts match best with experiment. The  $D_{2h}$  minimum geometry of B3LYP ( $\Delta r = 0$ ) most closely resembles the X-ray structure of TtB-s-indacene  $(\Delta r = 0.001 \text{ Å})$ , but the computed proton chemical shifts are significantly upfield shifted and far off from the experimental <sup>1</sup>H NMR data. Accordingly, NICS-XY-scans<sup>[17]</sup> computed for the  $D_{2h}$  B3LYP geometry of TtB-s-indacene show a higher paratropicity (more positive NICS values) compared to results obtained with the  $C_{2h}$  minimum geometries of M06-2X, ωB97X-D, and M11 (Figure 1C). Notably, the delocalization errors of B3LYP are less severe for a nonaromatic analogue of TtB-s-indacene. Computed proton chemical shifts for methyl-dihydro-TtB-s-indacene (Figure 1B) show a narrow spread (0.17 ppm for H8 and 0.11 ppm for H2) and the computed proton chemical shifts match better with <sup>1</sup>H NMR data for all functionals: B3LYP (H8: 7.41, H2: 6.40 ppm), M06-2X (H8: 7.49 ppm, H2: 6.34 ppm), ωB97X-D (H8: 7.47 ppm, H2: 6.30 ppm), and M11 (H8: 7.58 ppm, H2: 6.41 ppm) (cf. H8: 7.56 ppm, H2: 6.36 ppm, expt.).

Errors in predicting <sup>1</sup>H NMR shifts based on B3LYP geometries have been reported previously. [14,18-23] Choi and Kertesz noted that the proton chemical shifts of many higher annulenes, computed using geometries optimized at the B3LYP/6-31G(d) level, disagree with experiment. [15] Proton chemical shifts computed using B3LYP geometries for a porphyrin nanobelt structure reported by Anderson and Peeks in 2017 matched poorly with experimental <sup>1</sup>H NMR data. [21-24] The cause of this discrepancy is the large delocalization error of B3LYP. [25] Functionals like B3LYP have a low percentage of HF exchange at long interelectronic ranges and are prone to overestimating electron delocalization. [25] Such errors compromise theoretical inter-







pretations of the structures of large annulenes and extended  $\pi$ -conjugated macrocycles. We show here that the delocalization errors of B3LYP apply also to  $\pi$ -expanded antiaromatic systems and worsen for strongly antiaromatic species.

We chose to examine the performance of M06-2X,  $\omega$ B97X-D, and M11 because they represent a selection of the most commonly used DFT functionals in computational organic chemistry. These functionals are relatively efficient and suitable for studying large sets of expanded  $\pi$ -conjugated systems, and the increasing percentage of HF exchange in this set allows us to scrutinize the importance of long-range electron correlations for properly describing the geometries of antiaromatic compounds.

Besides computed NMR evidence, M06-2X, ωB97X-D, and M11 all predict a  $C_{2h}$  minimum structure for TtB-sindacene that is, respectively, 0.30, 0.57, and 1.49 kcal/mol lower in relative free energy ( $\Delta G_{\rm rel}$ ) than the  $D_{2h}$  transition state structure (Table 1). No  $C_{2h}$  minimum structure was found at the B3LYP/6-311+G(d,p) level. Since the barrier to interconverting the two equivalent  $C_{2h}$  structures of TtBs-indacene is small, dynamic disorder can give rise to a timeaveraged  $D_{2h}$  structure for room-temperature experiments and even for low temperature X-ray experiments. Eigenvectors of the imaginary frequencies for the  $D_{2h}$  transition state structure at M06-2X (645i cm<sup>-1</sup>),  $\omega$ B97X-D (688i cm<sup>-1</sup>), and M11 (1001i cm<sup>-1</sup>) are all substantial and indicate a strong tendency towards ring bond length alternation. CASSCF-(12,12)/6-311+G(d,p) calculations based on geometry optimization with an initial  $C_{2h}$  and  $D_{2h}$  symmetry both converged to a bond-alternating  $C_{2h}$  structure. Proton chemical shifts computed at CASSCF(12,12)/6-311G(d,p) for the  $C_{2h}$  structure (H8=6.74 ppm, H2=5.49 ppm) agreed moderately well with experiment (H8: 6.90 ppm, H2: 5.29 ppm).

Some electron-correlated methods predict a lower energy  $D_{2h}$  minimum for TtB-s-indacene. Single-point energies computed at DLPNO-CCSD(T)/def2-TZVP//M11/6-311 + G(d,p) predict a lower energy  $D_{2h}$  vs.  $C_{2h}$  structure ( $\Delta E_{rel}$  = 1.01 kcal/mol). Geometry optimizations at MP2/def-TZVP led to a  $D_{2h}$  structure; no  $C_{2h}$  structure was located. MP2/Def2-SVP computations also led to a single  $D_{2h}$  minimum structure; the lowest frequency corresponding to distortion towards  $C_{2h}$  symmetry is 145.9 cm<sup>-1</sup>. Computed proton chemical shifts for the MP2/def-TZVP geometry matched poorly with experimental values (H8: 6.63 ppm, cf. 6.90 ppm, expt.; H2: 4.84 ppm, cf. 5.29 ppm, expt.).

Indeed, the structure of TtB-s-indacene is a computational challenge. The small energy difference between the  $C_{2h}$  and  $D_{2h}$  structures are below the accuracy of many of the calculations reported above. Yet, a matched proton chemical shifts value for the  $C_{2h}$  structure provides definitive evidence. TtB-s-indacene may have a "quasi-delocalized" structure [8] with a competitive  $D_{2h}$  form, but the structure captured by Hafner's NMR experiments must have a  $C_{2h}$  symmetry.

During the course of this study, Cheng and Tobe et al. reported a series of substituted hexaaryl-s-indacenes with  $C_{2h}$ ,  $D_{2h}$ , and  $C_{2v}$  symmetries, as evidenced by X-ray measurements and calculations at the B3LYP level. [26] We

computed the symmetrically substituted hexaxylyl-s-indacene (compound **1f** in reference 26) and found that while hexaxylyl-s-indacene exhibits a  $D_{2h}$  s-indacene core at the B3LYP level, minimum geometries at the M06-2X,  $\omega$ B97X-D, and M11 levels show a  $C_{2h}$  s-indacene core. Computed proton chemical shifts based on M11 geometries give the best match with experiment (Figure 2).

Some of us recently published a joint experimental and theoretical study of indacenodibenzofurans (IDBFs).<sup>[27]</sup> We found that syn-IDBF shows a high degree of paratropicity exceeding that of the parent s-indacene, while anti-IDBF exhibits weaker paratropicity. Indeed, experimental <sup>1</sup>H NMR signals for the hydrogens on the central six-membered ring of syn-IDBF are shifted upfield (H<sub>svn</sub>: 5.60 ppm, Figure 3A) compared to those of anti-IDBF (H<sub>anti</sub>: 6.15 ppm, Figure 3B). Computed proton chemical shifts reproduce these trends, indicating a more antiaromatic syn-isomer. However, proton chemical shifts based on M11 geometries (H<sub>svn</sub>: 5.51 ppm, H<sub>anti</sub>: 6.04 ppm) are in much better agreement with experiment than those based on B3LYP geometries (H<sub>syn</sub>: 4.74 ppm, H<sub>anti</sub>: 5.74 ppm, note greater mismatch for the more antiaromatic syn-isomer) (see Figures 3A-3B and results for M06-2X and  $\omega B97X-D$  in the SI). These results suggest that M11 geometries most properly capture the degree of bond localization in syn- and anti- IDBF. Note the more bond alternated structures predicted by M11 ( $\Delta r_{svn} = 0.100 \text{ Å}, r_{anti} = 0.081 \text{ Å}$ ) compared to B3LYP geometries ( $\Delta r_{syn} = 0.047 \text{ Å}, \Delta r_{anti} = 0.004 \text{ Å}$ ).

In our previous study, NICS-XY-scans were computed using optimized B3LYP geometries of syn- and anti- IDBF. We now contrast these results to NICS-XY-scans obtained using M11 geometries. Figure 3C reproduces the published results[27] showing a higher paratropicity for syn-IDBF and a lower paratropicity for anti-IDBF, compared to the parent sindacene. NICS XY-scans based on M11 geometries (Figure 3D) confirm that syn-IDBF is more antiaromatic than anti-IDBF, but show in contrast to B3LYP results, that anti-IDBF is as antiaromatic as s-indacene based on comparisons of the NICS values at the five membered rings. Computations for indacenodibenzothiophenes (IDBT) and their sulfone analogues (IDBT-sulfone) are included in the SI, and further illustrate the limitations of predicting the <sup>1</sup>H NMR shifts and paratropicities of antiaromatic compounds based alone on B3LYP geometries.

M11 stands out as an especially suitable functional for the study of expanded  $\pi$ -conjugated [4n] antiaromatic

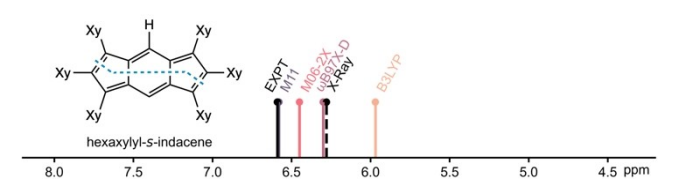


Figure 2. Experimental  $^1$ H NMR and computed proton chemical shifts for hexaxylyl-s-indacene (Xy=3,5-dimethylphenyl). Proton chemical shifts were computed at B97-2/6-311 + G(d,p) for minima geometries optimized at the B3LYP, M06-2X, ωB97X-D and M11/6-311 + G(d,p) levels and for a partially optimized X-ray structure.



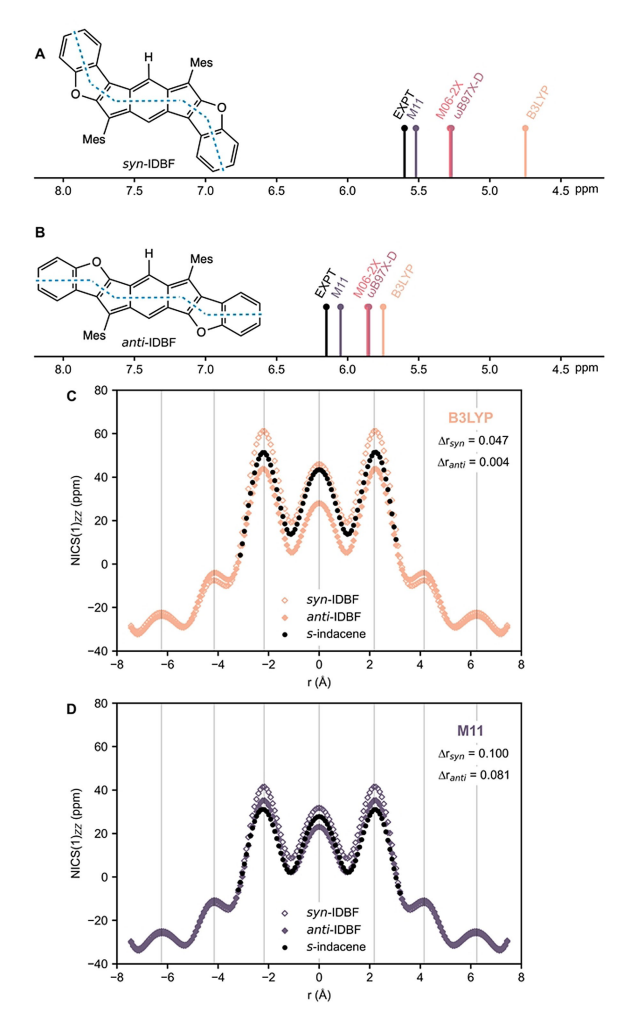


Figure 3. Experimental  $^1$ H NMR (data from reference [27]) and computed proton chemical shifts for the central hydrogens in A) syn-IDBF (H<sub>syn</sub>: 5.60 ppm, expt.) and B) anti-IDBF (H<sub>anti</sub>: 6.15 ppm, expt.). Computed NICS-XY-scans based on geometries optimized at the C) B3LYP and D) M11 levels. NICS-XY-scans for s-indacene using geometries optimized at the respective levels are included for comparison.  $\Delta r$  values indicate the difference between the two C–C bond lengths connected to C4/C8.

systems. Comparisons of experimental <sup>1</sup>H NMR measurements to ab initio NMR calculations for expanded pentalene cores also show that M11 geometries performs the best for describing the degree of bond localization in antiaromatic systems and therefore gives the closest match for proton chemical shifts. Tri-t-butyl-pentalene<sup>[28]</sup> shows a clear tendency for bond length alternation and experimental <sup>1</sup>H NMR measurements show highly shielded signals for the equivalent H1 and H3 protons and for H5 (H1/H3<sub>avg</sub>: 5.07 ppm, H5: 4.72 ppm, Figure 4A). Computed proton chemical shifts based on M11 geometries (H1/H3<sub>avg</sub>: 5.15 ppm, H5: 4.67 ppm) give a closer match with experiment compared to results based on B3LYP geometries (H1/ H3<sub>avg</sub>: 4.93 ppm, H5: 4.39 ppm). London et al. recently reported a series of substituted benzopentalenes (BP)[29,30] that can have two unique olefinic protons on the pentalene core. Computed proton chemical shifts for a selected BP

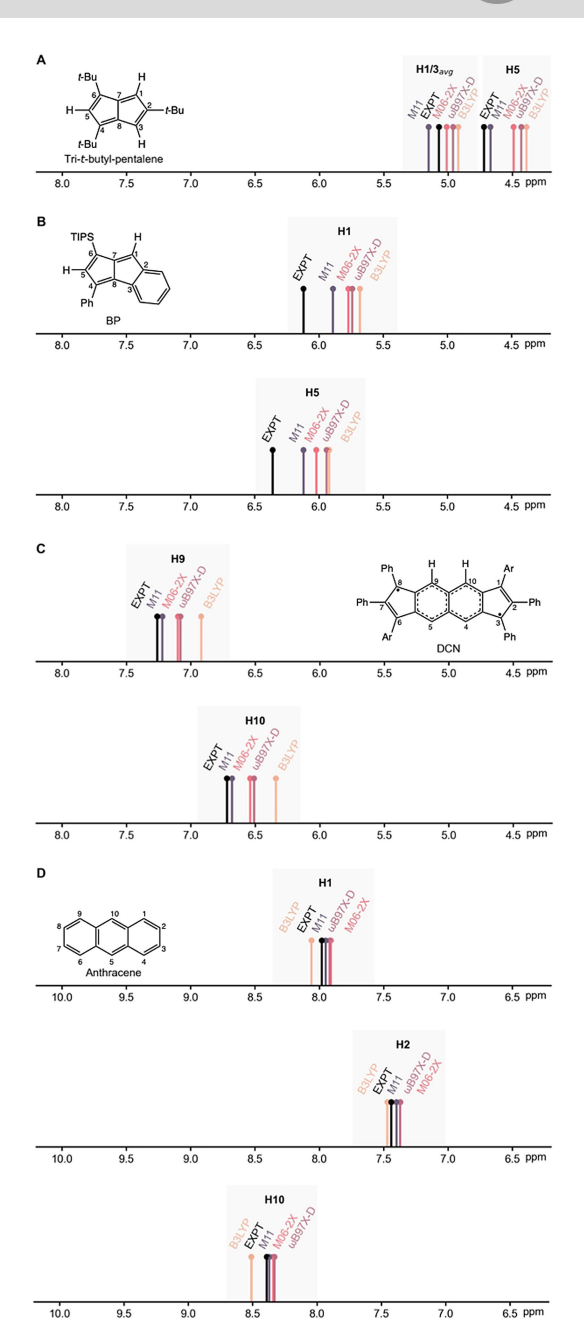


Figure 4. Experimental <sup>1</sup>H NMR and computed proton chemical shifts for: A) H1/H3<sub>avg</sub> and H5 in tri-t-butyl-pentalene (H1/H3<sub>avg</sub>· 5.07 ppm, H5: 4.72 ppm, expt., reference [28]), B) H1 and H5 in benzopentalene (H1: 6.12 ppm, H5: 6.36 ppm, expt., reference [29]), C) H9 and H10 in DCN (H9: 7.25 ppm, H10: 6.72 ppm, expt., reference [31]), and D) H1, H2, and H10 in anthracene (H1: 7.98 ppm, H2: 7.44 ppm, H10: 8.39 ppm, expt., reference [32]).

structure are shown in Figure 4B. Again, results based on M11 geometries (H1: 5.89 ppm, H5: 6.12 ppm) agree best with experimental <sup>1</sup>H NMR data (H1: 6.12 ppm, H5: 6.36 ppm), while computations based on B3LYP geometries give a poor match (H1: 5.68 ppm, H5: 5.94 ppm).

Another noteworthy example to examine is the dicyclopenta[*b*,*g*]naphthalene (DCN) derivative recently reported by Chi et al.<sup>[31]</sup> DCN is a core expanded *s*-indacene





isomer with pronounced open-shell singlet character ( $y_0$ = 0.30). Geometries of DCN were optimized with an unrestricted broken symmetry approach. As shown in Figure 4C, computed chemical shifts at the M11 geometry (H9: 7.23 ppm, H10: 6.68 ppm) match best with experimental <sup>1</sup>H NMR data (H9: 7.25 ppm, H10: 6.72 ppm). B3LYP geometries continue to perform poorly (H9: 6.92 ppm, H10: 6.34 ppm).

In contrast to their antiaromatic congeners, polycyclic aromatic hydrocarbons have bond delocalized  $\pi$ -systems and thus are *not* subject to the same problems inflicted by use of B3LYP geometries for studying magnetic properties. Computed proton chemical shifts for anthracene, based on geometries optimized at the B3LYP (H1: 8.06 ppm, H2: 7.47 ppm, H10: 8.51 ppm) and M11 (H1: 7.95 ppm, H2: 7.40 ppm, H10: 8.37 ppm) levels both show perfect agreement with experimental data (H1: 7.98 ppm, H2: 7.44 ppm, H10: 8.39 ppm) (Figure 4D).<sup>[32]</sup> Results for M06-2X and  $\omega$ B97X-D are included in the SI.

Polycyclic antiaromatic hydrocarbons like the  $\pi$ -expanded indacenes, indenofluorenes, pentalenes, cyclooctate-traenes, and cyclobutadienes [30,31,32-41] can show bond length alternation, strong paratropicity, and small HOMO-LUMO energy gaps, making them interesting candidates for organic electronics applications. [35,42-46] Yet, theoretical studies of these emerging antiaromatic species continue to rely largely on computations performed using the B3LYP functional. Herein we have shown that B3LYP geometries poorly capture the bond localizing features of polycyclic antiaromatic systems, and the errors are especially severe for highly antiaromatic systems. Highly electron-correlated methods like MP2 also can give over delocalized geometries for extended antiaromatic  $\pi$ -systems like the TtB-s-indacene.

#### Acknowledgements

J.I.W. thanks the National Science Foundation (CHE-1751370), the National Institute of General Medicine Sciences of the National Institutes of Health (R35GM133548), and the Alfred P. Sloan Research Foundation (FG-2020-12811) for support. M.M.H. thanks the National Science Foundation (CHE-1954389) for financial support. We thank the Research Computing Data Core at the University of Houston for computational resources.

#### **Conflict of Interest**

The authors declare no conflict of interest.

#### **Data Availability Statement**

The data that support the findings of this study are available in the supplementary material of this article. **Keywords:** Antiaromaticity  $\cdot$  B3LYP  $\cdot$  Density Functional Theory  $\cdot$  Expanded  $\pi$ -Conjugated Systems  $\cdot$  s-Indacene

- [1] K. Hafner, Pure Appl. Chem. 1982, 54, 939-956.
- [2] K. Hafner, B. Stowasser, H.-P. Krimmer, S. Fischer, M. C. Böhm, H. J. Lindner, *Angew. Chem. Int. Ed.* **1986**, *25*, 630–632.
- [3] E. Heilbronner, Z.-Z. Yang, Angew. Chem. Int. Ed. 1987, 26, 360–362.
- [4] J. D. Dunitz, C. Krüger, H. Irngartinger, E. F. Maverick, Y. Wang, M. Nixdorf, Angew. Chem. Int. Ed. 1988, 27, 387–389.
- [5] C. Gellini, G. Cardini, P. R. Salvi, G. Marconi, K. Hafner, J. Phys. Chem. 1993, 97, 1286–1293.
- [6] R. H. Hertwig, M. C. Holthausen, W. Koch, Z. B. Maksić, Angew. Chem. Int. Ed. 1994, 33, 1192–1194.
- [7] R. R. Hertwig, M. C. Holthausen, W. Koch, Z. B. Maksí, Int. J. Quantum Chem. 1995, 54, 147–159.
- [8] M. Nendel, B. Goldfuss, K. N. Houk, K. Hafner, J. Mol. Struct. 1999, 461–462, 23–28.
- [9] L. Moroni, C. Gellini, P. R. Salvi, J. Mol. Struct. 2004, 677, 1–5.
- [10] K. Hafner, K. H. Häfner, C. König, M. Kreuder, G. Ploss, G. Schulz, E. Sturm, K. H. Vöpel, *Angew. Chem. Int. Ed.* 1963, 2, 123–134.
- [11] T. Nakajima, T. Saijo, H. Yamaguchi, Tetrahedron 1964, 20, 2119–2124.
- [12] R. D. Brown, J. Chem. Soc. 1951, 2391-2394.
- [13] M. Bühl, P. v. R. Schleyer, J. Am. Chem. Soc. 1992, 114, 477–491.
- [14] C. S. Wannere, K. W. Sattelmeyer, H. F. Schaefer, III, P. v R. Schleyer, Angew. Chem. Int. Ed. 2004, 43, 4200–4206.
- [15] C. H. Choi, M. Kertesz, J. Chem. Phys. 1998, 108, 6681-6688.
- [16] K. K. Baldridge, J. S. Siegel, Angew. Chem. Int. Ed. 1997, 36, 745–748.
- [17] R. Gershoni-Poranne, A. Stanger, Chem. Eur. J. 2014, 20, 5673–5688.
- [18] H. M. Sulzbach, P. v. R. Schleyer, H. Jiao, Y. Xie, H. F. Schaefer, III, J. Am. Chem. Soc. 1995, 117, 1369–1373.
- [19] H. M. Sulzbach, H. F. Schaefer, III, W. Klopper, H. P. Lüthi, J. Am. Chem. Soc. 1996, 118, 3519–3520.
- [20] R. A. King, T. D. Crawford, J. F. Stanton, H. F. Schaefer, III, J. Am. Chem. Soc. 1999, 121, 10788–10793.
- [21] I. Casademont-Reig, R. Guerrero-Avilés, E. Ramos-Cordoba, M. Torrent-Sucarrat, E. Matito, Angew. Chem. Int. Ed. 2021, 60, 24080–24088.
- [22] J.-R. Deng, D. Bradley, M. Jirásek, H. L. Anderson, M. D. Peeks, Angew. Chem. Int. Ed. 2022, 61, e202201231.
- [23] I. Casademont-Reig, L. Soriano-Agueda, E. Ramos-Cordoba, M. Torrent-Sucarrat, E. Matito, Angew. Chem. Int. Ed. 2022, 61, e202206836.
- [24] M. D. Peeks, T. D. W. Claridge, H. L. Anderson, *Nature* 2017, 541, 200–203.
- [25] P. Mori-Sánchez, A. J. Cohen, W. Yang, Phys. Rev. Lett. 2008, 100, 146401.
- [26] S.-J. Jhang, J. Pandidurai, C.-P. Chu, H. Miyoshi, Y. Takahara, M. Miki, H. Sotome, H. Miyasaka, S. Chatterjee, R. Ozawa, Y. Ie, I. Hisaki, C.-L. Tsai, Y.-J. Cheng, Y. Tobe, J. Am. Chem. Soc. 2023, 145, 4716–4729.
- [27] J. E. Barker, T. W. Price, L. J. Karas, R. Kishi, S. N. MacMillan, L. N. Zakharov, C. J. Gómez-García, J. I. Wu, M. Nakano, M. M. Haley, Angew. Chem. Int. Ed. 2021, 60, 22385–22392.
- [28] K. Hafner, H. U. Süss, Angew. Chem. Int. Ed. 1973, 12, 575– 577.
- [29] T. Gazdag, P. J. Mayer, P. P. Kalapos, T. Holczbauer, O. El Bakouri, G. London, ACS Omega 2022, 7, 8336–8349.
- [30] P. J. Mayer, G. London, Org. Lett. 2023, 25, 42-46.
- [31] T. Xu, Y. Han, Z. Shen, X. Hou, Q. Jiang, W. Zeng, P. W. Ng, C. Chi, J. Am. Chem. Soc. 2021, 143, 20562–20568.





- [32] National Institute of Advanced Industrial Science and Technology, SDBSWeb, 2023, https://sdbs.db.aist.go.jp.
- [33] T. Nishinaga, T. Ohmae, K. Aita, M. Takase, M. Iyoda, T. Arai, Y. Kunugi, Chem. Commun. 2013, 49, 5354–5356.
- [34] C. Liu, S. Xu, W. Zhu, X. Zhu, W. Hu, Z. Li, Z. Wang, Chem. Eur. J. 2015, 21, 17016–17022.
- [35] C. K. Frederickson, B. D. Rose, M. M. Haley, Acc. Chem. Res. 2017, 50, 977–987.
- [36] Z. Jin, Z.-F. Yao, K. P. Barker, J. Pei, Y. Xia, Angew. Chem. Int. Ed. 2019, 58, 2034–2039.
- [37] J. Wang, M. Chu, J.-X. Fan, T.-K. Lau, A.-M. Ren, X. Lu, Q. Miao, J. Am. Chem. Soc. 2019, 141, 3589–3596.
- [38] C. K. Frederickson, L. N. Zakharov, M. M. Haley, J. Am. Chem. Soc. 2016, 138, 16827–16838.
- [39] J. J. Dressler, M. M. Haley, J. Phys. Org. Chem. 2020, 33, e4114.
- [40] T. Kawase, J.-i. Nishida, Chem. Rec. 2015, 15, 1045-1059.
- [41] B. Esser, J. S. Wössner, M. Hermann, Synlett 2022, 33, 737–753.
- [42] T. Kawase, T. Fujiwara, C. Kitamura, A. Konishi, Y. Hirao, K. Matsumoto, H. Kurata, T. Kubo, S. Shinamura, H. Mori, E.

- Miyazaki, K. Takimiya, *Angew. Chem. Int. Ed.* **2010**, *49*, 7728–7732.
- [43] J. L. Marshall, K. Uchida, C. K. Frederickson, C. Schütt, A. M. Zeidell, K. P. Goetz, T. W. Finn, K. Jarolimek, L. N. Zakharov, C. Risko, R. Herges, O. D. Jurchescu, M. M. Haley, *Chem. Sci.* 2016, 7, 5547–5558.
- [44] A. M. Zeidell, L. Jennings, C. K. Frederickson, Q. Ai, J. J. Dressler, L. N. Zakharov, C. Risko, M. M. Haley, O. D. Jurchescu, *Chem. Mater.* 2019, 31, 6962–6970.
- [45] R. Breslow, F. W. Foss Jr, J. Phys. Condens. Matter 2008, 20, 374104.
- [46] T. A. Su, M. Neupane, M. L. Steigerwald, L. Venkataraman, C. Nuckolls, Nat. Rev. Mater. 2016, 1, 16002.

Manuscript received: May 25, 2023 Accepted manuscript online: July 19, 2023 Version of record online: •••, •••





# **Communications**

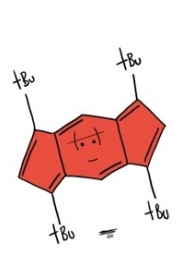
#### Computational Chemistry

L. J. Karas, S. Jalife, R. V. Viesser,

J. V. Soares, M. M. Haley,\*

j. l. Wu\* \_\_\_\_\_\_ e202307379

Tetra-tert-butyl-s-indacene is a Bond-Localized C<sub>2h</sub> Structure and a Challenge for Computational Chemistry





The structure of tetra-tert-butyl-s-indacene is a computational challenge. Highly correlated methods and popular DFT functionals predict a bond-delocalized  $D_{2h}$  symmetry, but excellent agreement between experimental and computed proton chemical shifts suggests a true  $C_{2h}$  geometry.



@JudyWuChem, @UOHaleyLab, @lucaskaras1, @SaidJalife, @RViesser, @\_joaovitoros

Share your work on social media! Angewandte Chemie has added Twitter as a means to promote your article. Twitter is an online microblogging service that enables its users to send and read short messages and media, known as tweets. Please check the pre-written tweet in the galley proofs for accuracy. If you, your team, or institution have a Twitter account, please include its handle @username. Please use hashtags only for the most important keywords, such as #catalysis, #nanoparticles, or #proteindesign. The ToC picture and a link to your article will be added automatically, so the tweet text must not exceed 250 characters. This tweet will be posted on the journal's Twitter account (follow us @angew\_chem) upon publication of your article in its final (possibly unpaginated) form. We recommend you to re-tweet it to alert more researchers about your publication, or to point it out to your institution's social media team.

Please check that the ORCID identifiers listed below are correct. We encourage all authors to provide an ORCID identifier for each coauthor. ORCID is a registry that provides researchers with a unique digital identifier. Some funding agencies recommend or even require the inclusion of ORCID IDs in all published articles, and authors should consult their funding agency guidelines for details. Registration is easy and free; for further information, see http://orcid.org/.

Dr. Lucas J. Karas http://orcid.org/0000-0001-7970-119X

Dr. Said Jalife http://orcid.org/0000-0003-0337-8730

Dr. Renan V. Viesser http://orcid.org/0000-0002-4176-6067

João V. Soares http://orcid.org/0000-0002-7070-8376

Prof. Michael M. Haley http://orcid.org/0000-0002-7027-4141

Prof. Judy I. Wu http://orcid.org/0000-0003-0590-5290